ORIGINAL PAPER

Comparison of high-resolution and dynamic reaction cell ICP-MS capabilities for forensic analysis of iron in glass

Waleska Castro · Tatiana Trejos · Benjamin Naes · José R. Almirall

Abstract Forensic laboratories routinely conduct analysis of glass fragments to determine whether or not there is an association between a fragment(s) recovered from a crime scene or from a suspect to a particular source of origin. The physical and optical (refractive index) properties of the fragments are compared and, if a "match" between two or more fragments is found, further elemental analysis can be performed to enhance the strength of the association. A range of spectroscopic techniques has been used for elemental analysis of this kind of evidence, including inductively coupled plasma mass spectrometry (ICP-MS). Because of its excellent sensitivity, precision, and accuracy, several studies have found that ICP-MS methods (dissolution and laser-ablation) provide the best discrimination between glass fragments originating from different sources. Nevertheless, standard unit-resolution ICP-MS instruments suffer from polyatomic interferences including $^{40}Ar^{16}O^+$, $^{40}Ar^{16}O^1H^+$, and refractory oxide $^{40}Ca^{16}O^+$ that compromise measurements of trace levels of Fe^{56+} and Fe^{57+}, for example. This is a drawback in the analysis of glass fragments because iron has been previously identified as a good discriminating element. Currently, several techniques are available that enable reduction of such interferences. However, there are no data comparing detection limits of iron in glass using those techniques. The aim of this study was to compare, the analytical performance of high-resolution sector field inductively coupled plasma mass spectrometry (HR-SF-ICP-MS) and quadrupole ICP-MS equipped with a dynamic reaction cell (DRC-ICP-MS), for the detection of iron in glass, in terms of accuracy, precision, and method detection limits (MDLs). Analyses were conducted using conventional acid-digestion and laser-ablation methods. For laser-ablation analyses, carrier gases were compared to assess the effect on detection limits in the detection of iron isotopes. Iron polyatomic interferences were reduced or resolved by using a dynamic reaction cell and high-resolution ICP-MS. MDLs as low as 0.03 $\mu g\ g^{-1}$ and 0.14 $\mu g\ g^{-1}$ were achieved in laser-ablation and solution-based analyses, respectively. Use of helium as carrier gas improved detection limits for both iron isotopes in medium-resolution HR-SF-ICP-MS and in DRC-ICP-MS.

Keywords Glass · Elemental analysis · DRC-ICP-MS · HR-SF-ICP-MS · Forensic

W. Castro · T. Trejos · B. Naes · J. R. Almirall (✉)
Department of Chemistry and Biochemistry and International
Forensic Research Institute (IFRI), Florida International University,
11200 SW. 8th Street,
Miami, FL 33199, USA
e-mail: almirall@fiu.edu

Introduction

The fragile nature of glass and its abundance in our surroundings makes glass a common type of evidence found at crime scenes such as hit-and-run accidents, burglaries, shootings, and other violent crimes. Vehicle windows, architectural windows, headlamps, and containers are the major sources of glass evidence. Forensic examiners typically begin by screening the evidence by measuring physical and optical properties such as color, thickness, fluorescence, and refractive index, and by microscopic examination [1–12]. If a match between known and questioned fragments is found in this preliminary stage, elemental analysis is typically conducted in order to improve the discrimination value of the analysis. When two or more fragments share a common elemental profile, they can be considered to originate from the same manufacturing source and provide strong scientific evi-

dence associating a person with an event or two objects with each other. Fragments found to differ by elemental content can be determined to originate from different manufacturing sources and also provide useful information to the court or investigators.

A variety of trace elemental analysis techniques have been used for this purpose, including atomic absorption spectroscopy (AAS) [13–15], X-ray fluorescence (XRF) [16, 17, 19], neutron activation analysis (NAA) [18], scanning electron microscopy with energy dispersive X-ray detection (SEM-EDX) [19, 20], inductively coupled plasma atomic emission spectrometry (ICP-AES) [8, 11, 21–24], and inductively coupled plasma mass spectrometry (ICP-MS) [25–28]. Each technique has its own advantages and shortcomings. ICP-MS has been shown to be the most effective analytical method for comparison of the trace elements in small glass fragments due to its multi-element capability, excellent sensitivity, high sample throughput, and the capability to provide isotopic information.

Physical evidence, especially trace evidence, can sometimes provide a significant breakthrough in a criminal investigation by linking an individual to the crime. This trace evidence is often found at the sub-microscopic level (typically 0.1–1 mm), therefore in forensic laboratories it is necessary to employ reliable analytical approaches that also minimize sample consumption. Although conventional digestion methods for ICP-MS have been shown to be excellent tools for elemental analysis of glass these have the disadvantage of requiring complete sample dissolution, therefore destroying the sample, prior to introduction to the ICP-MS and also increasing the risk of contamination through the use of acids. During the last two decades, laser ablation (LA) has increasingly been used and preferred as a sample-introduction method in forensic laboratories, because of its advantages over dissolution of the glass prior to analysis [29–32]. The most significant advantages of LA sampling include the capability of spatial resolution and in-situ spot analysis, small sample consumption, reduction in sample preparation time, shortened analysis time, and reduced risk of contamination. These advantages make LA a suitable sampling technique for analysis of trace evidence such as glass and paint in forensic cases.

Variations in elemental profiles within glass populations are because of differences in elemental composition of the raw materials used and/or those contributed by the manufacturing processes. Although some of the raw materials used in glass manufacture are relatively pure, a glass product may contain impurities, such as iron oxide, that could produce undesirable color and alter furnace temperatures. Only one-part-per-thousand of iron oxide in sand can impart a green color to the glass and therefore manufacturers usually use decoloring agents to remove or mask the tint. Iron oxide is typically present at concentrations that range from 0.07 to 0.16% (w/w) in float glass,

0.03 to 0.15% (w/w) in containers, 0.05% (w/w) in borosilicate glass, and 0.01% (w/w) in lead crystal glass while in optical and insulating lead glasses iron oxide content is reduced to trace levels [33].

The elements used for discrimination of glasses by ICP-MS have been critically selected from previous studies in which precision, accuracy, and discrimination potential of these elements were evaluated at major, minor, and trace levels [25, 26]. Iron has been identified in previous studies as an excellent discriminating element and it has been successfully used for classification and discrimination of glasses by X-ray fluorescence spectroscopy [8, 16, 34] and ICP-AES [8, 34]. Nevertheless, the concentration of iron in some glass populations may be close to or lower than the limits of detection of XRF and ICP-AES. Although standard ICP-MS methods provide better sensitivity than the aforementioned techniques, analytical performance for iron is a challenge because of inherent interferences. In 2000, Duckworth et al. reported that elements measured by ICP-MS without good bias ($\leq 10\%$) and precision ($\leq 10\%$ RSD) were closely inspected before using them as discriminating elements in a database for float glass. In this study bias and precision for iron were higher than 10% [6]. The poor precision and accuracy of iron measurements in glass standards do not allow its use in glass databases and limits its use in casework.

The challenges in analysis of iron in glass by ICP-MS are the result of polyatomic isobaric interferences such as $^{40}Ca^{16}O^{+}$ and $^{40}Ar^{16}O^{+}$ on $^{56}Fe^{+}$, and $^{40}Ca^{16}O^{1}H^{+}$, $^{40}Ar^{16}O^{1}H^{+}$, and $^{41}K^{16}O^{+}$ on $^{57}Fe^{+}$. Fortunately, there are several ICP-MS techniques capable of resolving polyatomic interferences. These interferences can be suppressed by using either DRC or HR [35–37]. In solution-based analysis using DRC-ICP-MS, MDLs in 2% HNO_3 and in a rain water/HNO_3/HF matrix were compared; detection limits reported by Frontier Geosciences Laboratories (Seattle, WA, USA) were as low as 9 ng L^{-1} for the 2% HNO_3 sample and 383 ng L^{-1} for the rainwater sample [38]. Balcaen et al. performed determinations of Fe in $AgNO_3$ solutions with isotope dilution using the DRC-ICP-MS with NH_3 as reactant gas. They reported lower iron detection limits with isotope dilution (0.013 μg g^{-1}) than with external calibration (1.2 μg g^{-1}) [39]. In 2001 Günther et al. reported a comparison of detection limits of $^{56}Fe^{+}$ and $^{57}Fe^{+}$ using the standard (STD) mode and the DRC mode with hydrogen and neon as reactant and buffer gases, respectively, for laser-ablation experiments. The limits of detection were determined for a spot size of 40 μm using the gas blank and ablation of SRM NIST 610 glass. In that study, the limits of detection were improved from 5.9 μg g^{-1} in STD mode to 2.1 μg g^{-1} using DRC mode for $^{57}Fe^{+}$, while for $^{56}Fe^{+}$ the limits of detection were reported to be 0.3 μg g^{-1} [40].

A study of trace elements in quartz by LA-HR-ICP-MS, with external calibration with the three SRMs, NIST 612, NIST 614, and NIST 616, reported limits of detection for $^{56}Fe^+$ of 2.6 µg g^{-1} in medium mass resolution [41]. Iron detection limits of the order of pg g^{-1} were reported for analyses of water, plant, tissue, and rock samples in medium mass resolution by HR-SF-ICP-MS. The MDLs for iron in oyster tissue/tomato leaves and rock sample digestion blanks were reported to be 113 pg g^{-1} and 3940 pg g^{-1}, respectively, for $^{56}Fe^+$, and 580 pg g^{-1} and 10600 pg g^{-1} for $^{57}Fe^+$ [42].

Although there are reports of iron detection limits with both ICP-MS systems, at present there are no data comparing detection limits for $^{56}Fe^+$ and $^{57}Fe^+$ in glass samples using those techniques and utilizing both laser ablation and solution-introduction methods. The capability of resolving or reducing the iron polyatomic interferences by using the DRC and high-resolution systems will enable more optimized use of Fe for discrimination of glass samples.

This work was conducted to evaluate the method detection limits (MDL) that can be achieved for Fe using different ICP-MS systems (quadrupole, dynamic reaction cell, and high resolution) for solution and laser-ablation sample-introduction methods of glass standard reference materials (SRMs). This work includes assessment of precision and accuracy for iron measurements to evaluate the possibility of including iron in routine forensic analyses of glass samples by ICP-MS.

Experimental

Laser ablation analysis

Glass standard reference material (SRM) NIST 612 (National Institute of Standards and Technology, Gaithersburg, MD, USA) was used for laser-ablation analyses with both ICP-MS systems using all configurations. SRM NIST 610 (National Institute of Standards and Technology, Gaithersburg, MD, USA) and the FGS glass standards described elsewhere [43] were used as external calibrators for some experiments using a NewWave UP 213 laser-ablation system (Fremont, CA, USA) and argon as the carrier gas. Method detection limits were calculated for $^{56}Fe^+$ and $^{57}Fe^+$ using SRM NIST 612. Standard reference materials (SRMs) NIST 1831, NIST 614, and the FGS standards were analyzed to evaluate the accuracy and precision of the method. For proper assessment of LA experiments using the Element 2 high-resolution ICP-MS (Thermo Electron, Bremen, Germany) and the Elan DRC II (Perkin-Elmer, LAS, Shelton, CT, USA), other SRMs were used in place of SRM 612 because the former was used as an external calibrator in the data-reduction analyses. For

practical purposes only the results for SRM FGS1 will be presented for all the laser-ablation ICP-MS systems.

The total analysis time was of approximately 170 s. During the first 55 s the laser was blocked (via the use of a shutter) and the signal of the "blank" was acquired in order to take the background level into account. The laser was then fired for 60 s, but only the middle-latter 40 seconds of the ablation signal were used for measurements, because of the inherent instability caused when the laser first interacts with a sample. Following these 60 s the laser was turned off and the signal was recorded for an additional 55 s to purge any signal carryover between samples. Seven sample replicates of SRM NIST 612 on two non-consecutive days were used to determine the MDLs of LA analyses. Figure 1 shows the transient signal of $^{56}Fe^+$ during a typical analysis. The Glitter software (Glitter, Gemoc, Macquarie University, Australia) was used for data reduction to determine concentration and the MDLs. Glittter software enables plotting of the transient signal collected from the LA analysis and selection of the background and signal intervals for data reduction. To determine the concentration the Glitter software uses Eq. 1, where $conc_{ni}$ is the concentration of element i in analysis n, cps_{nij} is the mean count rate (background subtracted) of isotope j of element i in analysis n, $abundance_j$ is the natural abundance of isotope j, and $yield_{ni}$ is the cps per ppm of element i in analysis n. The $yield_{ni}$ is calculated using Eq. 2, where $yield_{ns}$ is the cps per ppm of the internal standard s in analysis n, $Int(yield_{ni}/yield_{ns})^{std}$ is the ratio of the yield of element i in analysis n to the yield of the internal standard s in analysis n interpolated over the standard analyses.

$$conc_{ni} = (cps_{nij}/abundance_j)/(yield_{ni}) \qquad (1)$$

$$yield_{ni} = yield_{ns} * Int(yield_{ni}/yield_{ns})^{std} \qquad (2)$$
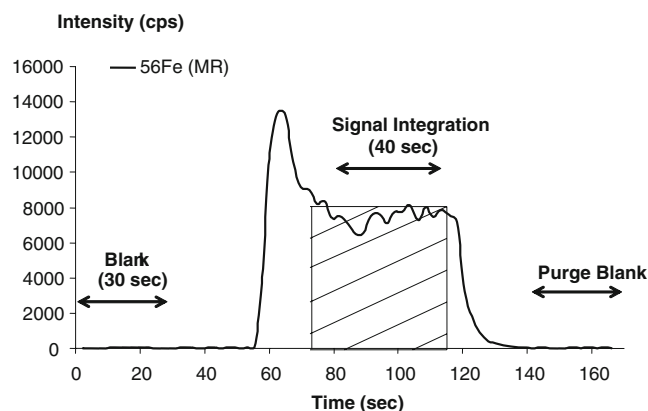

Fig. 1 A typical laser-ablation transient signal of iron of mass 56 in SRM NIST 612 analyzed with the Element 2

Glitter software uses Eq. 3 to calculate the limits of detection with a 99% confidence level on the basis of Poisson counting statistics. In Eq. 3 *B* is the total counts in the background interval.

$$MDL = 2.3 \times *\sqrt{2B} \tag{3}$$

The LA data analysis was performed using SRM NIST 612, SRM 610, or SRM FGS2 as a single-point external calibrator. For all the analytical determinations ^{29}Si was used as the internal standard, except for the DRC experiments where ^{24}Mg was chosen as the internal standard.

The glass SRMs were rinsed with high-purity deionized water and dried overnight prior to LA analysis.

Solution analysis

High-purity standards (CPI International, Santa Rosa, California, USA) were used for the preparation of the external calibration curves. Optima-grade nitric acid (HNO_3), hydrofluoric acid (HF), and hydrochloric acid (HCl) (Fisher Scientific Pittsburg, USA) were used for acid digestion. High purity deionized water (18 MΩ cm^{-1}) and HNO_3 were used for sample dilution and for the preparation of the calibration curve solutions. Rhodium was used as internal standard for all solutions analyzed.

To determine the accuracy and precision of the analysis, SRMs NIST 612, NIST 1831, NIST 614 (National Institute of Standards and Technology, Gaithersburg, MD, USA) and standards FGS1 and FGS2 were digested in accordance with the ASTM E2330–04 standard method for trace elemental analysis of glass by ICP-MS [27].

The samples were washed first in methanol for 10 min, then with 1.6 mol L^{-1} HNO_3 for 30 min, followed by rinsing with high-purity water (>18 MΩ cm^{-1}). After rinsing, they were left to dry overnight. Glass samples were crushed and weighed to approximately 2 mg $\pm$ 1 μg into 5-mL polypropylene tubes. Optima grade HNO_3, HF and HCl were used for digestion of glass. Samples were sonicated for 2 h before the drying process in the dry heater block (Dry Digital Bath Incubator; Boekel Scientific, Feasterville, PA, USA). After the samples were taken to complete dryness, they were reconstituted with 0.8 mol L^{-1} HNO_3, the internal standard, and high-purity water. Dilutions of the reconstituted digested glass samples were prepared and measured with seven reagent blanks that were treated in the same way as the glass samples.

The calibration curves were prepared from single-element high-purity standards (1000 μg g^{-1}) (CPI International, Santa Rosa, California, USA). Rhodium was added as internal standard to final concentrations 3 ng g^{-1}, 3 ng g^{-1}, and 50 ng g^{-1} for the HR-SF-ICP-MS, DRC mode ICP-MS, and standard mode ICP-MS calibration curves, respectively.

Calibration curves had seven calibration points in the ranges 0–10 ng g^{-1} for the Element 2 and Elan DRC Mode, and 0–100 ng g^{-1} for Elan STD mode analyses. Two control verification checks (at 3 and 5 ng g^{-1} for Element 2 and Elan DRC mode and at 7 and 25 ng g^{-1} for the Elan standard mode) were run with samples in order to evaluate drift and precision over time. All sample preparations and analyses were performed in a normal laboratory environment.

The glass samples were measured against an external calibration curve. The intensities (cps) for the standards and samples were normalized to the rhodium (internal standard) signal (cps). A linear regression line was determined from the plot of the normalized signal (cps) against the concentration of the correspondent standard, and the concentrations in the samples were determined by using the slope and intercept of this equation.

The iron MDLs in solution analyses of SRM NIST 612 were determined by using the standard deviation of the blank's signal and the slope of the calibration curve. MDLs were determined with at least seven replicates of reagent blanks measured on two non-consecutive days in order to account for inter-day variations.

In order to compare the MDLs obtained from laser and solution work, the MDLs for solution are referred to the concentration on glass assuming an average weight of 2 mg of glass diluted to 4 mL after acid digestion [27]. Therefore, MDL obtained in μg L^{-1} were multiplied by a factor of 2 to be reported in μg g^{-1} on glass.

Precision and accuracy of LA and solution analysis

The accuracy of the analyses was determined by comparing the experimental values for iron with the certified and/or consensus values for SRMs NIST 612 and NIST 1831, and standards FGS1 and FGS2. Precision was determined by calculating the relative standard deviation (%RSD) of five sampling replicates for each glass sample. The method was evaluated with an accuracy of ≤10% bias from the consensus or certified value, and precision of ≤10% RSD.

Instrumentation

Laser systems

Two different Nd:YAG laser units were used for this work:

1. a New Wave UP-213 operating at 213 nm (New Wave Research, Fremont, CA, USA); and
2. a Cetac LSX 200+ (Cetac Technologies, Omaha, NE, USA) operating at 266 nm.

Laser ablation settings are further described in Table 1. The laser ablation systems were operated under different

conditions using both helium and argon as carrier gases, and different ablation cell volumes. The experimental conditions were optimized for each system.

ICP-MS systems

The ICP-MS instruments used for this study were an Elan DRC II ICP-MS (Perkin-Elmer, LAS, Shelton, CT, USA) and a HR-SF-ICP-MS ThermoFinnigan Element 2 (Thermo Electron, Bremen, Germany). The DRC-ICP-MS was equipped with a quartz cyclonic spray chamber and a concentric tube pneumatic nebulizer. The sample-intake rate into a concentric nebulizer and cyclonic spray chamber was 1 mL min^{-1} An ASX 510 autosampler (Cetac Technologies) was coupled to the ICP-MS for the solution analyses. For laser-ablation analyses, the laser systems were connected to the torch intake of the ICP-MS. The DRC-ICP-MS was operated in STD mode and DRC mode. The removal of $^{56}Fe^+$ polyatomic interferences was achieved by using methane as reactant gas in the DRC mode. Methane is often used as reactant gas for removal Fe interferences [44, 45]. Preliminary results in our laboratory showed better sensitivity of detection of $^{56}Fe^+$ with methane as reactant gas. Removal of the refractory interference CaO^+ in the glass matrix was significantly better with methane than with other gases. It seems that methane works better for removal of $^{56}Fe^+$ interference CaO^+ from Ca-rich matrices. Additionally, for safety reasons, it is more convenient to work with methane than with ammonia gas. For solution analyses the HR-SF-ICP-MS sample-introduction setup included a quartz cyclonic spray chamber with a microflow PFA-ST nebulizer (400 μL min^{-1} intake flow) (ESI Scientific, Omaha, NE, USA) and a 1.5 mm quartz injector connected to a CD-type quartz torch as a removable injector (ESI Scientific). The laser systems were connected to a 1.75 mm quartz injector inserted into the torch. The HR-SF-ICP-MS system was used in the three mass resolutions available— low ($R \approx 300$), medium ($R \approx 4,000$), and high ($R \approx 10,000$).

Before conducting each experiment, the instruments were optimized for sensitivity (maximum counts per second) and for doubly-charged species ($\leq 3\%$) and oxides ($\leq 0.3\%$). Additional optimization in LA analyses of the ratio U/Th for SRM 612 was also conducted as a measure of fractionation levels (with $\sim 1 \pm 0.2$ determined to be acceptable).

Results and discussion

Three main ICP-MS configurations were used to evaluate the method detection limits for iron in glass analysis: ICP-MS STD mode, ICP-MS DRC mode, and HR-SF- ICP-MS, where the latter two were used to reduce the polyatomic

Table 1 Instrument settings used for the MDL experiments

Laser system			ICP-MS system			
Parameters	CETAC LSX 200+	New wave UP 213	Parameters	ELAN DRC II (STD mode)	ELAN DRC II (DRC mode)	ELEMENT 2
Wavelength	266 nm	213 nm	Auxiliary Gas	1.1 L min^{-1}	1.0 L min^{-1}	10.8 L min^{-1}
Spot Size	100 μm	100 μm	Carrier gas	0.90 L min^{-1} (laser, He) 0.80 L min^{-1} (laser, Ar)	0.90 L min^{-1} (laser, Ar)	0.60–0.72 L min^{-1} (laser, Ar) 1.0–1.1 L min^{-1} (laser, He)
Energy Output	4.8 mJ	2.4 mJ	Nebulizer Flow	1.0 L min^{-1} (solution)	1.0 L min^{-1} (solution)	1.0 L min^{-1} (solution)
Repetition Rate	10 Hz	10 Hz		0.98 L min^{-1} (laser)	0.98 L min^{-1} (laser)	0.62–0.70 L min^{-1} (laser)
Carrier gas	Ar or He	Ar or He	RF Power	1500 W (solution) 1550 W (laser)	1501 W (solution) 1550 W (laser)	1300 W (solution) 1350 W (laser)
Ablation Cell Volume	50.2 mL	30.0 mL	Reaction Gas	–	CH4	–
			Reaction Gas Flow	–	0.5 L min^{-1}	–
			RPq	–	0.5 (laser) 0.6 (solution)	–
			Resolution Modes	–	–	Low, Medium and High

–Not applicable

Table 2 Accuracy (%Bias) and precision (%RSD) for solution-based analyses of standard FGS1

Isotope	ELAN STD mode			ELAN DRC mode			E2 in MR			E2 in HR		
	(Ave) ± σ	%RSD	[b] %Bias	(Ave) ± σ	%RSD	[b] %Bias	(Ave) ± σ	%RSD	[b] %Bias	(Ave) ± σ	%RSD	[b] %Bias
^{57}Fe	699±9	1.3	21	–	–	–	544±52	10	6	529±13	3	9
^{56}Fe	–	–	–	554±58	10	5	542±61	11	7	521±10	2	10

[a] Average (Ave) concentration in $\mu g\ g^{-1}$
[b] Bias was determined using the consensus value of Fe: 580±60 $\mu g\ g^{-1}$ [30]
–Not determined

interferences associated with Fe measurements. MDLs were evaluated for laser-ablation and solution modes, because these are the two major sample-introduction methods routinely used in forensic laboratories for elemental analysis. Two laser systems were used with helium and argon, separately, as carrier gases in order to account for the effects of laser wavelengths on sensitivity. The ablation process and the efficiency of transportation of particles into the ICP-MS are important factors affecting sensitivity and limits of detection. It is been reported that use of helium as carrier gas has improved sensitivity and limits of detection for several trace elements [46, 47]. Table 1 shows the experimental conditions used for each ICP-MS configuration.

Both isotopes ^{56}Fe$^+$ and ^{57}Fe$^+$ were analyzed, however the target isotope in this study was ^{56}Fe$^+$, because it is of greater abundance than ^{57}Fe$^+$ (91.72% vs 2.2%). Iron interferences are an analytical challenge for standard ICP-MS systems because polyatomic interferences containing argon (a property of the ICP) and calcium (a major component in glass) are present at very high levels.

Method evaluation for solution-based and laser-ablation analysis

Analytical performance of DRC vs. STD mode

Analytical performance of the method was evaluated in terms of limits of detection, accuracy, and precision. For solution analysis in STD mode, ^{57}Fe$^+$ concentration in the standard FGS1 was much higher than the consensus value meaning the interferences present were not efficiently removed in this mode, possibly because of high abundances of argon hydroxide interferences. This effect of the interferences in standard mode is more pronounced at low concentration levels of iron, as in the case of SRM 612, in which iron is only present at 56.3 $\mu g\ g^{-1}$. By using the DRC mode, the iron interferences were properly reduced, leading to accurate measurement of ^{56}Fe$^+$ compared with the consensus value (580±60 $\mu g\ g^{-1}$) with bias and precision less than 10% (Table 2). The target mass to reduce interferences in DRC with methane is iron of mass 56 for

Table 3 Accuracy (%Bias) and precision (%RSD) for laser-ablation analyses of standard FGS1

Isotope	(Ave) ± σ	%RSD	[b] %Bias	(Ave) ± σ	%RSD	[b] %Bias	(Ave) ± σ	%RSD	[b]%Bias
(ELEMENT 2 -New Wave UP213 laser)									
	E2 in LR (Ar)			**E2 in MR (Ar)**			**E2 in HR (Ar)**		
^{57}Fe	557±25	5	4	619±5	1	7	630±8	1	9
^{56}Fe	–	–	–	629±11	2	8	636±22	3	10
(ELEMENT 2 –New Wave UP213 laser)									
	E2 in LR (He)			**E2 in MR (He)**			**E2 in HR (He)**		
^{57}Fe	631±15	6	9	602±17	3	4	561±39	3	3
^{56}Fe	–	–	–	609±23	2	5	556±8	2	4
(ELEMENT 2 –CETAC LSX 200+)									
	E2 in LR (Ar)			**E2 in MR (Ar)**			**E2 in HR (Ar)**		
^{57}Fe	613±14	2	6	650±13	2	12	565±4	1	3
^{56}Fe	–	–	–	641±3	0.5	11	648±5	1	12
(ELEMENT 2 –CETAC LSX 200+)									
	E2 in LR (He)			**E2 in MR (He)**			**E2 in HR (He)**		
^{57}Fe	561±16	3	3	613±22	4	6	544±40	7	6
^{56}Fe	–	–	–	547±16	3	6	636±12	2	10

[a] Average (Ave) concentration in $\mu g\ g^{-1}$
[b] Bias was determined using the reference value of Fe: 580±60 $\mu g\ g^{-1}$ [30]
–Not determined

Table 4 MDLs for laser-ablation analyses of $^{56}Fe^+$ and $^{57}Fe^+$ using different ICP-MS systems

Isotope	MDLs ± σ μg g^{-1} (ELEMENT 2 -LSX 200+ laser)			MDLs ± σ μg g^{-1} (ELEMENT 2 -New Wave UP213 laser)			MDLs ± σ μg g^{-1} (ELEMENT 2 -New Wave UP213 laser)						MDLs ± σ μg g^{-1} (ELAN DRC II -New Wave UP213 laser)			
	LR (Ar)	MR (Ar)	HR (Ar)	LR (He)	MR (He)	HR (He)	LR (Ar)	MR (Ar)	HR (Ar)	LR (He)	MR (He)	HR (He)	STD mode (He)	STD mode (Ar)	DRC mode (He)	DRC mode (Ar)
^{57}Fe	2.3±0.1	0.40±0.04	1.5±0.5	2.4±0.1	0.23±0.06	1.2±0.6	8.3±0.9	0.9±0.4	3.6±0.6	3.5±0.3	0.8±0.2	3.9±1.2	9.5±1.0	9.6±2.0	–	–
^{56}Fe	–	0.055±0.003	0.15±0.01	–	0.037±0.003	0.11±0.03	–	0.12±0.01	0.3±0.1	–	0.085±0.007	0.29±0.05	–	–	a 0.025±0.003	0.6±0.2

a Data published from a previous study [37]

– Not determined

its possible application to routine forensic analysis of glass. Iron of mass 57 was not measured in DRC mode; therefore the effect of reducing the main interferences with this mass was not optimized. In LA analyses in STD mode and with different carrier gases, $^{57}Fe^+$ produced better accuracy than in solution-based analyses. This is because in LA mode the dry plasma contains much less hydroxide interference from species such as $^{40}Ca^{16}O^1H^+$ and $^{40}Ar^{16}O^1H^+$. For analysis of $^{56}Fe^+$ in DRC mode the interferences were efficiently reduced leading to good accuracy with <10% bias and measurement precision of <10% RSD (Table 3).

Analytical performance of HR-SF-ICP-MS in different resolution modes

Interferences of $^{57}Fe^+$ were not properly resolved for solution analyses with the Element 2 in low-resolution mode because of the larger amount of hydroxides present in the wet plasma. Hydroxide species $^{40}Ca^{16}O^1H^+$ and $^{40}Ar^{16}O^1H^+$ in solution-based analyses of $^{57}Fe^+$ in LR mode contributed to the significant increase in its measured concentration compared with the consensus value for FGS1. Therefore the results for iron of mass 57 in LR mode were not reported. The accuracy and precision of $^{57}Fe^+$ measurements were improved in medium-resolution (MR) and high-resolution (HR) modes, with less than 10% bias and less than 10% RSD for precision (Table 2).

For most of the laser-ablation experiments using HR-SF-ICP-MS with the three mass resolutions, polyatomic interferences with $^{56}Fe^+$ and $^{57}Fe^+$ were properly resolved providing accurate concentration measurements of iron in the standard FGS1. Accuracy and precision of the analyses at all mass resolutions were within the acceptable limits (≤10% bias and ≤10% RSD) (Table 3).

In general, solution-based and laser-ablation accuracy and precision results with the different ICP-MS configurations were in agreement. The results showed improved accuracy in DRC mode. For HR-SF-ICP-MS, medium resolution was the optimum setting for $^{56}Fe^+$ measurement. The method was properly assessed giving validity to the MDL results obtained during these experiments.

Method detection limits of solution-based and laser-ablation analysis

The iron method detection limits in DRC mode were significantly lower than in standard mode (0.03 vs 9.5 μg g^{-1} for laser-ablation analysis and 0.33 vs 1.9 μg g^{-1} for solution-based analysis). This demonstrates the ability of the DRC to eliminate interferences and reduce limits of detection, leading to more certainty in iron determinations in glass matrices. Higher background levels in solution and laser-

Table 5 MDLs for solution analyses of $^{56}Fe^+$ and $^{57}Fe^+$ using different ICP-MS systems

Isotope	MDLs ± σ for Solution Analyses in µg g^{-1} (ELEMENT 2)		MDLs ± σ for Solution Analyses in µg g^{-1} (ELAN DRC II)	
	E2 in MR	E2 in HR	ELAN STD mode	ELAN DRC mode
^{57}Fe	0.19±0.12	0.58±0.10	1.9±1.2	–
^{56}Fe	0.14±0.06	0.62±0.11	–	0.30±0.04

–Not determined

ablation analyses in STD mode contribute to higher detection limits of $^{57}Fe^+$.

The use of a high-resolution sector-field ICP-MS resolved polyatomic interferences of iron. Low MDLs for both iron isotopes were achieved in laser-ablation analyses using the Element 2, particularly in medium-resolution mode, for $^{56}Fe^+$. Higher MDLs in HR mode could be attributed to the increase in resolution which reduces the sensitivity, therefore affecting the limits of detection (Table 4). When comparing the MDLs results in MR and HR modes using the two laser systems, higher detection limits were observed with the NW UP213 laser system. The differences in the ablation process including laser energy and the amount of mass ablated could contribute to such MDL variations. Regardless, the MDL values are comparable (Table 4). In low-resolution mode, high background levels contributed to the observed increase in detection limits. This pattern was also observed for the STD mode of the quadrupole instrument.

In solution-based analyses with the HR-SF-ICP-MS improved MDLs for both iron isotopes were obtained in medium and high-resolution modes vs. low-resolution. In the quadrupole system, the DRC enabled achievement of MDLs of 0.30 µg g^{-1} for $^{56}Fe^+$ (Table 5). In MR and HR modes, the interference signals were properly separated from the iron signals, whereas in DRC mode the polyatomic interferences are significantly reduced by chemical reaction but may not be completely removed.

In solution-based analyses higher MDLs were obtained for $^{56}Fe^+$ than with laser ablation. Differences in the MDLs could be attributed to the dilution factor and the background contributions associated with the digestion process.

Effect of carrier gas on laser ablation MDLs with the Element 2 and Elan DRC II ICP-MS systems

MDLs for both iron isotopes obtained with the Cetac LSX 200+ laser coupled to the HR-SF-ICP-MS were not significantly different at low and high resolution when argon or helium were used as the carrier gas. Slightly lower MDLs were obtained for $^{56}Fe^+$ and $^{57}Fe^+$ when helium carrier gas was used in medium-resolution mode. Experiments per-

formed with the New Wave UP 213 laser coupled to the HR-SF-ICP-MS resulted in similar MDLs for $^{57}Fe^+$ and $^{56}Fe^+$ with helium and argon carrier gases in medium and high-resolution modes. In low-resolution mode higher MDLs were obtained when using argon as carrier gas, because of the higher background produced with this laser of lower energy (2.4 mJ vs. 4.8 mJ for the Cetac LSX 200+).

With the Elan DRC II, the carrier gas effect was more significant. Lower detection were achieved when helium was used as the carrier gas. MDLs determined for iron isotopes with the Elan DRC II with both carrier gases were comparable with those observed in MR with the Element 2 with both laser-ablation systems/carrier gas combinations.

For laser-ablation analysis of the glass matrix, helium as carrier gas has been proved to increase the sensitivity in the detection of elements. The improvement in sensitivity is attributed to more efficient particle removal and transportation into the ICP-MS [46, 47]; therefore lower detection limits are achievable.

Conclusions

Polyatomic interferences for iron were significantly reduced or resolved with both DRC-ICP-MS and HR-SF-561ICP-MS. Method limits of detection as low as ~0.03 µg g^{-1} were achieved with both DRC and the SF instruments using laser-ablation mode for glass matrices (Table 4). DRC-ICP-MS is an excellent tool for achieving low MDLs for Fe in both laser-ablation and solution analyses, but is limited to analysis of few elements in the DRC mode, because suppression of interferences is chemically dependent and other interferences that affect the analysis could be formed in the dynamic reaction cell. From a practical point of view, this limitation requires separate measurements for Fe and for the other elements typically used in glass comparisons, especially when LA is involved, because the transition from DRC to non-DRC mode is not fast enough for transient signals. The need to perform separate analysis for Fe and for the rest of the elements used in glass analysis is not only time-consuming but also requires more sample. An advantage of DRC-ICP-MS over HR-SF-ICP-MS is its lower cost and its ease of use.

HR-SF-ICP-MS enabled resolution of iron interferences in both medium and high-resolution modes. In laser ablation lower MDLs were achieved by use of medium resolution because in high-resolution mode the sensitivity is significantly reduced. In solution analyses, the HR-SF-ICP-MS system at MR results in lower detection limits than DRC-ICP-MS (0.14 μg g^{-1} vs. 0.30 μg g^{-1}, respectively). Advantages of HR-SF-ICP-MS over DRC-ICP-MS instruments include its capability to achieve lower MDLs for Fe (particularly for laser-ablation sample introduction) and its capability to conduct multielemental analysis using laser ablation. Nevertheless, the fast transient signal measured in laser ablation does not allow switching between different resolution modes in the same method, therefore multi-elemental analysis is restricted to one resolution mode in the sector field instrument. The detection limits of some elements may be affected in medium and high-resolution modes, because increasing the resolution means sacrificing analytical sensitivity. These are important factors when considering use of laser ablation with the sector field instrument.

Solution and LA analyses with the different ICP-MS instrumental setups enabled accurate and precise measurement of the iron isotopes. The accuracy and precision in multielemental analysis could be affected when the DRC-ICP-MS is used. The reactant gas could react with other isotopes of interest within the glass matrix causing problems in their detection. Although similar MDLs can be achieved with helium or argon as carrier gas in the LA-HR-SF-ICP-MS systems, lower detection limits could be obtained with helium.

This work demonstrates the capabilities of these ICP-MS systems and setups to resolve and/or reduce polyatomic interferences, enabling accurate and precise measurement of iron isotopes in glass matrices. Although there were some differences in MDLs for each of the LA setups and ICP-MS systems, these results open the possibility of doing elemental analysis which includes use of iron isotopes in routine casework analysis of glass.

References

1. Pearce NJ, Perkins WT, Westgate JA, Gorton MP, Jackson SE, Neal CR, Chenery SP (1997) Geostandard Newslett 21:115–144
2. Brown G (1985) J Forensic Sci 39:806–813
3. Almirall JR, Cole M, Gettinby G, Furton K (1998) Sci Justice 38:93–100
4. American Society for Testing Materials (2003) (E1967–98 R03) Standard test method for the automated determination of refractive index of glass samples using the oil immersion method and a phase contrast microscope. In: ASTM Annual Book of ASTM Standards, vol 14.2. American Society for Testing Materials, West Conshohocken, PA, p 664
5. Locke J (1987) Microscope 35:151
6. Duckworth DC, Bayne CK, Morton DJ, Almirall JR (2000) J Anal At Spectrom 15:821
7. Montero S, Hobbs AL, French TA, Almirall JR (2003) J Forensic Sci 48:1101–1107
8. Koons RD, Peters CA, Rebbert PS (1991) J Anal At Spectrom 6:451
9. Parouchais T, Warner IM, Palmer LT, Kobus II (1996) J Forensic Sci 41:351
10. Almirall JR (2001) Manslaughter caused by a hit and run: glass as evidence of association. In: Ilouck, M (eds) Mute witness: trace evidence analysis. Academic Press, San Diego, CA, p 139
11. Buscaglia J (1994) Anal Chim Acta 288:17–24
12. Thornton JI, Langhauser C, Kehane D (1984) J Forensic Sci 29:711
13. Catterick T, Wall C (1978) Talanta 25:573–577
14. Catterick T, Hughes J, Southeard G (1976) J Forensic Sci 8:217–227
15. Almirall JR (2001) Elemental analysis of glass fragments. In: Caddy, B (eds) Forensic examination of glass and paint. Taylor and Francis, London, pp 65–83
16. Ryland S (1986) J Forensic Sci 31:1314
17. Dudley RJ, Howden CR, Taylor TJ, Smalldon KW (1980) X-ray Spectrum 9:119
18. Coleman RF, Goode GC (1973) J Radioanal Chem 15:367–388
19. Jembrih D, Schreiner M, Peev M, Krejsa P, Clausen C (2000) Mikrochim Acta 133:151–157
20. Zadora G, Brozek-Mucha Z (2003) Mater Chem Phys 81:345–348
21. Andrasko J, Maehly A (1978) J Forensic Sci 23:250–262
22. Hickman DA (1981) Forensic Sci Int 17:265
23. Hickman DA (1987) Forensic Sci Int 33:23
24. Almirall JR (1998) PhD thesis, University of Strathclyde, UK
25. Suzuki Y, Sugita R, Suzuki S, Marumo Y (2000) Anal Sci 16:1195
26. Zurhaar A, Mullis L (1990) J Anal At Spectrom 5:611
27. American Society for Testing Materials (2004) (E2330–04) Standard test method for the determination of trace elements in glass using inductively coupled plasma mass spectrometry. In: ASTM annual book of ASTM standards, vol 14.2. American Society for Testing Materials, West Conshohocken, PA, p 1
28. Beary ES, Paulsen P (1993) Anal Chem 65:1602–1608
29. Trejos T, Montero S, Almirall JR (2003) Anal Bioanal Chem 376:1255–1264
30. Latkoczy C, Becker S, Ducking M, Günther D, Hoogewerff JA, Almirall JR, Buscaglia J, Dobney A, Koons RD, Montero S, van der Peijl GJQ, Stoecklein WRS, Trejos T, Watling JR, Zdanowicz VS (2005) J Forensic Sci 50:1327–1341
31. Watling RJ, Lynch BF, Herring D (1997) J Anal At Spectrom 12:195–203
32. Bajic SJ, Aeschliman DB, Saetveit NJ, Baldwin DP, Houk RS (2005) J Forensic Sci 50:1123–1127
33. Copley J, Almirall JR (1999) In: Caddy B (ed) Forensic examination of glass and paint, chap 2, 4. Taylor and Francis, London, pp 39, 67
34. Koons RD, Fieldler C, Rawalt RC (1988) J Forensic Sci 33:49–67
35. Nonose NK (2001) J Anal At Spectrom 16:560–566

36. Weyer S, Schwieters JB (2003) Int J Mass Spectrom 226:355–368
37. Umpierrez S, Trejos T, Neubauer K, Almirall J (2006) At Spectrosc 27:76–79
38. Gürleyük H, Brunette RC, Howard CR, Schneider C, Thomas R (2005) Spectroscopy 20:22–29
39. Balcaen L, Geuens I, Moens L, Vanhaecke F (2003) Anal Bioanal Chem 377:1020–1025
40. Günther D, Hattendorf B, Audétat A (2001) J Anal At Spectrom 16:1085–1090
41. Flem B, Larsen RB, Grimstvedt A, Mansfeld J (2002) Chem Geol 182:237–247
42. Townsend AT (2000) J Anal At Spectrom 15:307–314
43. Becker S, Ducking M, Watzke P, Stoecklein W (2003) Forensic Sci Int 136:361
44. Hill SJ, Ford MJ, Ebdon L (1992) J Anal At Spectrom 7:1157–1165
45. Rowan JT, Houk RS (1989) Appl Spectrosc 43:976–980
46. Günther D, Heinrich CA (1999) J Anal At Spectrom 14:1363–1368
47. Horn I, Günther D (2003) Applied Surface Sci 207:144–157